EFFECT OF BLANK HOLDER FORCE ON DRAW FORMING OF STEEL/SRPP FIBRE METAL LAMINATE

J. Nam[a*], W. Cantwell[b], R. Das[c], A. Lowe[a], S. Kalyanasundaram[a]

[a]*Research School of Engineering, Australian National University, Canberra, 0200, Australia*
[b]*Centre for Materials and Structures, University of Liverpool, L69 3BX Liverpool, United Kingdom*
[c]*Department of Mechanical Engineering and Centre for Advanced Composite Materials, University of Auckland, Auckland*
**jae.nam@anu.edu.au*

Keywords: Fibre Metal Laminate, Real-time strain measurement system, Stamp forming, Forming limit diagram.

Abstract

This paper presents findings on forming and wrinkling behaviour of Fibre Metal Laminate system based on steel and self-reinforced polypropylene composite material systems. Stamp forming experiments were conducted at room temperature with a hemispherical punch under different blank holder forces. Resulting surface strains were captured real-time using a 3D photogrammetric measurement system, from which forming limit diagrams could be constructed. Increase in blank holder force resulted in reduced severity of wrinkling and larger formable depth, except at the largest blank holder force for which inter-laminar delamination occurred and lower forming depth was reached. More stretching as opposed to drawing occurred with larger blank holder forces and along axes at 0°/90° to fibre orientations of the composite material.

1. Introduction

Exponential advancements in mass production of gasoline and diesel driven vehicles have undoubtedly benefited many in present society but have also raised ubiquitous concerns about its adverse impacts on the environment. In view of the increasing climate change and demand for non-renewable resources outstripping supplies, people are now facing an ever-increasing oil price and a seemingly impossible task of limiting greenhouse gas emission levels. Currently, car manufacturers are making every effort to meet what German Association of the Automotive Industry called “the most severe targets in the world” [1] set by the European Commission. It requires the fleet average of all new passenger cars to not exceed 95 grams of carbon dioxide emission per kilometre (g/km) by 2021, which amounts to a 40% reduction from 2007 fleet average of 158.7 g/km [2]. Similar targets have been set for the US (93 g/km for 2025), Japan (105 g/km by 2020) and China (117 g/km by 2020) [3].

Driven by incentives and substantial penalties involved with these targets, manufacturers have already been on the move to replace traditional steel parts by lighter alternatives, such as aluminium, ultra-high-strength steels and composite materials. One of the most recent examples is the new Volkswagen XL1 Super Efficient Vehicle which is currently in

production [4]. It utilises carbon fibre reinforced polymer and a new resin transferring moulding technique. Joining the fast developments in venturing into novel ways of reducing vehicle weight, researches have taken place recently to investigate the feasibility of adopting Fibre Metal Laminates (FMLs) for manufacturing body parts of automobiles.

FML is a hybrid system consisting of alternating layers of fibre-reinforced composite and metal, mainly aluminium. Conventional methods of manufacturing with FMLs are too expensive in terms of time and cost for mass production, due to the use of composites based on thermoset matrix which have to be formed in its final shape. This has led to researches in FMLs using thermoplastic-based composites. As thermoplastics can be reshaped under increased temperature and have larger strain to failure than thermosets, they can be pre-consolidated into sheets and formed subsequently by stamp forming, which is a forming process widely used for mass production of sheet metal components in automotive manufacturing. This was first demonstrated by Hou et al. in 1994, who conducted 3D stamp forming of pre-consolidated sheets of a thermoplastic-based composite [5].

Since its debut, various stamp forming investigations have been carried out on thermoplastic-based composites. Lim et al. worked on determining the amount of stretching relative to drawing in stamp forming of Kevlar-reinforced polypropylene (PP) and suggested the importance of the tool profile, blank size and Blank Holder Force (BHF) on sheet formability [6]. There have also been studies on stamp forming of composites based on carbon-fibre and polyether-ether-ketone [7] and on flax-fibre and PP [8]. Cabrera et al. studied non-isothermal stamp forming of 'all-PP' or Self-Reinforced PP (SRPP), in which both the fibres and matrix are PPs. It was shown that intra-ply shear was the dominant mode of deformation, as with Glass-Fibre-Reinforced PP (GFRP), but requiring less energy to deform [9].

Based on these researches which illustrate good formability of PP-based composites, several advancements have been made during the last decade, in investigating into formability of aluminium FMLs based on the composites. Mosse studied the inter-laminar load transfer and effects of process parameters on cup and channel forming with SRPP and GFRP-based FMLs, showing improved formability compared to that of monolithic aluminium [10-12]. Gresham researched into draw forming of the same FML and verified the importance of having controlled temperature and sufficient BHF [13]. Studies on channel and stretch forming of SRPP-based FMLs demonstrated its potential for mass production via stamp forming, as well as superior formability than aluminium or steel with optimal process parameters [14,15], effects of which were further studied in draw forming [16].

The FML systems used in the mentioned studies utilise aluminium as the metal layer. To broaden the current spectrum of knowledge, the authors have proposed forming with steel FMLs.

2 Experimental Procedures

2.1 Material and Specimen Preparation

For the preparation of a FML, a 1.0mm thick SRPP sheet (0.9g/cm^3) was glued between two

sheets of steel 0.45mm thick each (7.85g/cm^3) using hot-melt film adhesives. The SRPP used was Curv®, manufactured by Propex Fabrics using hot compaction of PP tapes woven in a twill weave pattern. For steel and adhesive, GALVABOND® G2 from BlueScope Steel and Collano® 22.010, a thin thermoplastic adhesive film based on modified polyolefins, were used. The adhesive has a minimum bonding temperature of 130ºC and a density of 0.9g/cm^3.

Constitutive layers were cut to 210 x 240 mm rectangles, stacked and placed in a platen press at 145ºC. The layers were held together with minimal pressure for 5 minutes to allow the adhesives to reach its melting temperature, and then pressured at 1.2MPa for further 5 minutes to ensure good adhesion. The laminate was then rapidly cooled to 35ºC over the course of approximately 7 minutes to form a steel/SRPP FML approximately 1.95mm thick. The FML was then cut into a circular blank with a diameter of 180mm.

2.2 Experimental setup

In draw forming of a circular FML blank, a 300kN double-action mechanical press with hydraulic ram was used. The blank was placed on an open die with a diameter of 105mm and held against the die with a pneumatic blank holder of the same diameter. The specimen was then deformed with a semi-hemispherical punch with 100mm diameter, driven at a feed rate of 20 mm/s into the die until a 10% drop in the load cell was detected, in anticipation of failure of the blank at the maximum force. A thin sheet of polytetrafluoroethylene was placed between the punch and the specimen for lubrication. BHF was varied to investigate its effect on forming, from 0kN (no blank holder) to 2kN, 7kN and 14kN, with three repeats at each test except at 0kN which was tested once.

A 3D photogrammetric measurement system (ARAMIS) developed by GOM mbH was used for analysing strains on the surface of the blank that is not in contact with any tool. ARAMIS operates on gathering optical data via two high-resolution digital cameras at high speed and performing 3D image correlation on the data to give full field strains.

3 Results and Discussions

3.1 Wrinkling and Delamination Behaviour

For all the specimens, most noticeable behaviours were wrinkling around edges and delamination, albeit in different degrees. Overall, decrease in severity of wrinkling was observed with increase in BHF, as can be seen in Figure 1. As the flange region of a blank cannot be observed during forming due to the die obstructing the view, forming depths were recorded when wrinkling could be detected by ARAMIS at the die edge.

Without any blank holder (0kN), a large wrinkle appeared in the FML before folding over onto itself. At 2kN BHF, wrinkling occurred at the die edge but with no significant fold. For both 0kN and 2kN BHFs, blanks continued to form after wrinkling to deeper depths, until maximum load was reached, causing the wrinkles to be flattened between the punch and the die wall. Because of this, height of the wrinkles could not be measured but observations showed that smaller wrinkles formed with 2kN BHF. Similarly, height of wrinkles continued to decrease with increase in the BHF to 7kN and 14kN, exhibiting maxima of 7±1mm and

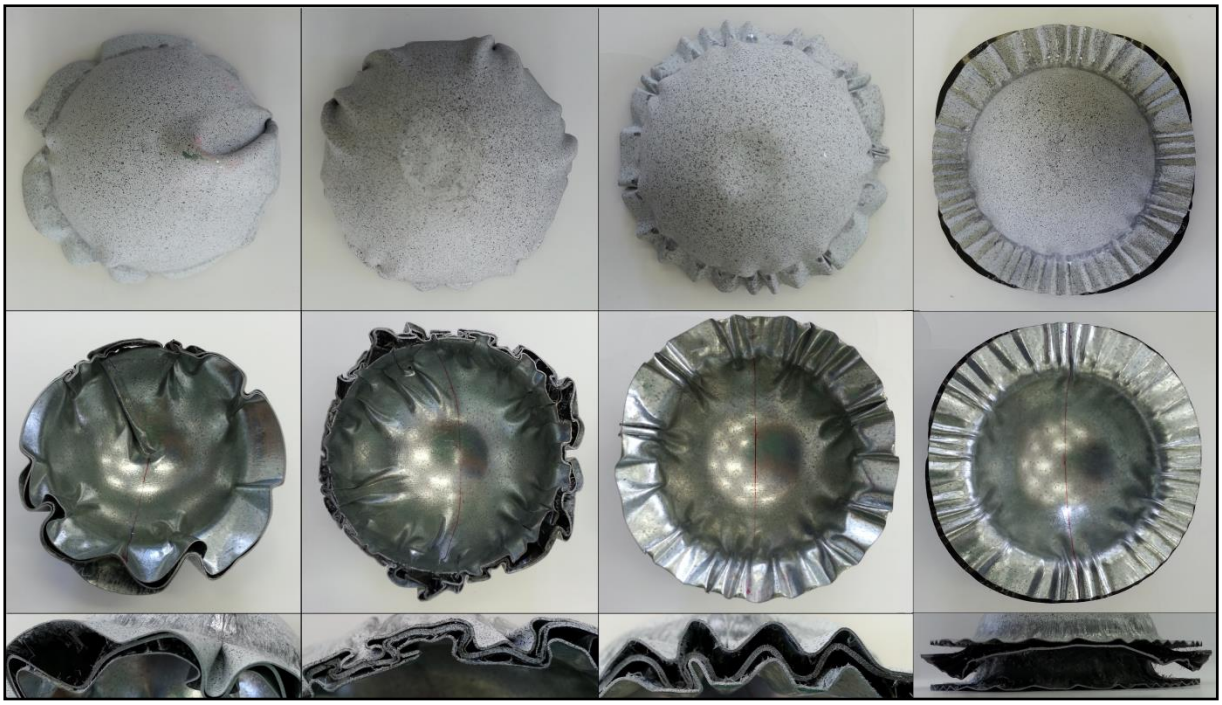

Figure 1. Wrinkling and delamination in steel/SRPP FMLs formed under blank holder forces of a) 0kN (no blank holder), b) 2kN, c) 7kN and d) 14kN. Top, middle and bottom rows show outer parts, inner parts and edges of the formed FML domes respectively.

2.5±0.5mm respectively. At larger BHF, frequency or the number of wrinkles was increased but its propagation from the flange area towards the centre of the dome was decreased, showing more control over wrinkling or less defect in the region of interest.

As for the depth the domes could be formed to before wrinkling, there was a substantial increase when the BHF was raised from 0kN to 2kN, reaching depths of 5.58mm and 17±5mm respectively. This amounts to an increase by a factor of 3. With 7kN BHF, twice the depth at BHF of 2kN could be reached, at 37±2mm. Such trend indicates that formability of the FML may be increased by using a larger BHF. However, at 14kN, the forming depth decreased slightly to 33.8±0.6mm. This may be due to either a) the wrinkling occurring at a smaller depth at 7kN but not being detected due to the die obstructing the view, or b) the larger BHF causing more stretch along the fibres which in turn causes inter-ply delamination or separation of the layers at earlier stages.

Partial delamination was observed in one of the specimens tested at 7kN BHF, which had its inner steel layer (in contact with the punch) de-bonded completely from the SRPP layer. With specimens tested at 14kN BHF, all three layers have separated from each other, as the one shown in Figure 2, except for one specimen which was partially adhered in some parts. From the delaminated 14kN specimens, it could be observed that the SRPP had drawn into the die to a larger degree along the lines where the fibres pass through centre of the blank in the direction of the fibres, compared to the material along the lines passing through the centre at 45º to the fibre directions. (Figure 2a.) This can be attributed to resistance of the fibres to stretching causing the material to draw into the die at a greater extent along the fibre directions, as the punch pulls the fibres in contact with it into the die, whereas trellising of the fibres allow more elongation of the material along the 45º lines. Trellising is in-plane shearing

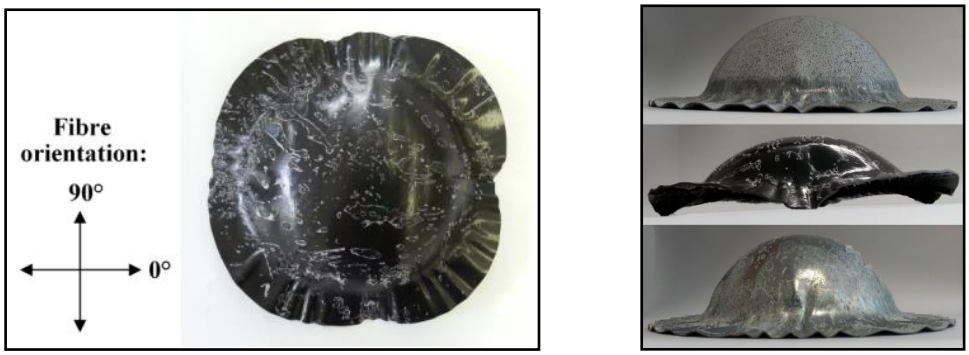

Figure 2. Delaminated layers of a steel/SRPP FML formed under 14kN blank holder force: a) SRPP layer, b) outer steel layer, SRPP layer and inner steel layer at top, middle and bottom of the figure, respectively.

caused by fibres moving over each other within the ply in such a way that the fibres are no longer perpendicular to each other, when tension is applied off-axis to the fibres.

As the trellising of the fibres increase length of the material along the direction of the radial tension and more deformation is allowed in the matrix than along the fibres, SRPP is more stretched than drawn along 45º to the fibres. The result is round-square shaped SRPP layer which is approximately 4% shorter in diameter along the fibres than at 45º to it, and slightly more rounded steel layers with approximately 3% difference in diameters along 0º and 45º to the SRPP fibres. Such difference in diameters is not observed in specimens tested at lower BHFs, suggesting that 7kN and below are insufficient to hold down the blank to the extent of stretching the fibres.

It is worth noting that the degree the fibres are bent through at the die edge is greater along the fibres passing through the centre, and more force is required along these lines. The difference in the amount draw and the degree of bending of the fibres along 0º/90º and 45º/45º lines have resulted in significant warping in the flange of the composite layer (average amplitude of 6.5±0.3mm), and is illustrated in Figure 2. Stress state in the material causing warping is such that it caused delamination from the outer steel layer at the flange along the 0º/90º lines in the partially delaminated 7kN specimen, while the two layers remain intact at the flange along the diagonals. There is also less wrinkling of the FML at the flange in the 45º/45º directions.

It appears that SRPP is the limiting material in forming of the FML under given conditions. The delaminated SRPP have sprung back to a lower depth, as shown in Figure 2b, indicating that the steel layers have been driving the forming to respective depths. In a specimen that was formed to a depth of 49±1mm, SRPP layer had sprung back by 14%, to a depth of 42±1mm. Interestingly, maximum height of the wrinkles was larger in steels (2.5mm) than in SRPP (2mm), suggesting that wrinkling is driven by steel layers. As for non-delaminated specimens at 7kN and at lower BHFs, inter-ply delamination could only be seen along some parts of the edges but because any sizable dent put on the dome centre of the outer steel did not affect the inner steel layer, it could be deduced that inter-ply delamination occurred at the centre. Since SRPP had significant spring-back in delaminated specimens, it seems more likely that the delamination occurred between the composite and outer steel layer. It may be that the wrinkles which have been compressed together between the punch and the die wall, as those shown in Figures 1a~c, are holding the laminas together, despite the delamination.

Another observation was that SRPP fibres were pulled out of the plane due to delamination such that undulating patterns could be seen, mostly along the 45º/45º lines, at points from about 30mm from the centre into the flange region, suggesting larger inter-laminar shear at these points. Formability of the FML may be improved at higher temperature as this would allow the fibres to stretch further, as well as reduce intra-ply delamination within SRPP which could be seen along the edge of the specimens, especially where wrinkles appeared.

3.2 Forming Limit Diagram

A Forming Limit Diagram (FLD) shows surface strain distribution of a formed part prior to failure. Figure 3 illustrates FLDs for steel/SRPP FMLs at different BHFs, with elliptical envelope indicating strains where wrinkling occurs soon after. Strain ratio, β, is a ratio of minor strain to major strain, often used to describe deformation modes of an element.

Observing the FLDs in Figure 3 shows that the FML experiences a wide range of deformation modes on its outer surface, from equal biaxial stretching (β=1) at the centre, to drawing at the edge (β= -1), with the area in-between experiencing transitioning deformation modes. FLD of the FML with no BHF (Figure 3a), illustrates that failure occurred at points along the surface experiencing draw and compression (β< -2) deformations. Interestingly, there were points with larger minor strain which did not wrinkle first. This was also observed in other samples and demonstrates the difficulty in predicting wrinkling. With BHF of 2kN (Figure 3b), main modes of deformation were biaxial stretch in the centre and draw along the edges where wrinkling occurs, as indicated by the ellipse in the FLD.

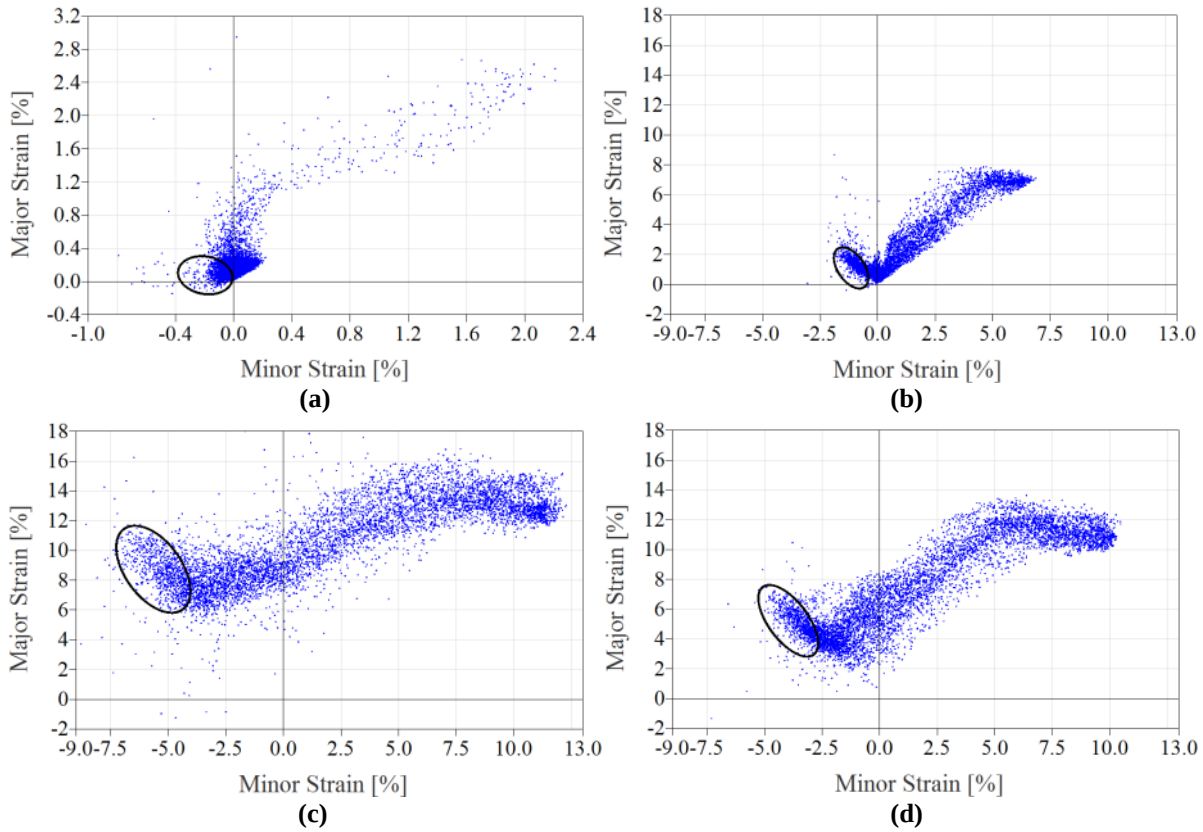

Figure 3. Strain distribution over surface of outer steel of steel/SRPP FMLs prior to failure during draw forming with blank holder forces of a) 0kN (no blank holder), b) 2kN, c) 7kN and d) 14kN. Elliptical envelops indicate where wrinkling is about to occur.

Although specimens were formed to greater depth with 7kN and 14kB BHFs, strain distributions at forming depths of approximately 19mm were studied at these BHFs for comparison to results with 2kN. Similar strain distributions could be seen to that of the FLD at 2kN BHF, but with more concentration of points along draw and biaxial stretch and less along plane strain deformation. As the BHF increased from 2kN to 7kN, there was an overall decrease in magnitude and in number of points along draw and a corresponding increase along biaxial deformation. Also, the strain distribution became more concentrated along a narrower band towards equal biaxial stretch and the maximum β shifted slightly from approximately 0.9 to 1. These reflect that increase in BHF causes an overall shift in forming modes to more stretching and less drawing, which verifies the hypothesis drawn from the previous section. Also, at 7kN, there was an increase in irregular points which were high in magnitude (in both major and minor strains) and/or at compressive state beyond drawing.

For specimens formed with 14kN BHF at similar depth, similar strain distributions could be observed as at 7kN, except for a slight change in the deformation modes of edge points, with β changing from approximately -0.9 to -0.8. Again, this verifies the general shift in the forming mode from draw to stretch with increase in BHF. However, there was a slight decrease in magnitude of maximum major and minor strains along biaxial deformation, contrary to the trend with increased BHF. Number of points under compressive strains also increased again, although wrinkling did not necessarily occur at such points.

FLDs at final stages of forming before wrinkling at BHFs 7kN (Figure 3c) and 14kN (Figure 3d) show that larger strains could be tolerated compared to when formed with smaller BHF, although wrinkling occurs at $\beta \approx -0.7$ regardless of the change in BHFs. The decrease in level of strains with increase in the BHF from 7kN to 14kN may be explained by the fact that 7kN specimens could be formed to larger depth. At 7kN BHF, the strain distribution is more even, meaning that the difference in strain states between neighbouring regions of the blank is more gradual. Therefore, it can be deduced that increase in the formable depth is ideal in this aspect, which would require careful control over processing parameters.

4 Conclusions

This research investigated into stamp forming of SRPP-based steel FMLs at room temperature. Observational and real-time strain measurement techniques were used to analyse how the FML forms under varying BHFs. Wrinkling occurred in all samples but in a less severe manner at larger depths with increased BHF in general. At the largest BHF tested, inter-ply delamination occurred, with spring-back and warping of the SRPP layer. The layer exhibited more stretching along the fibres passing through the centre compared to lines at 45^o to this, which experienced trellising allowing more drawing. FLDs generated showed spread in surface strain deformation modes from equal biaxial stretch to compression, as well as illustrate the increase in magnitude of the strains, slight transition from draw to stretch and more gradual spread in deformation modes, with increase in BHF. It must be kept in mind that increase in BHF reduce the degree of wrinkling but induce inter-ply delamination above a certain value which limits the forming depth. It is therefore suggested that future research consist of larger BHF and high temperature, so that wrinkling is minimised while forming depth may be increased with softer composite layer.

References

[1] V. Mock, 25 February 2014. 'European Parliament Agrees Tough Automobile CO2 Targets', *The Wall Street Journal*, viewed 10 March 2014, http://online.wsj.com/news/-articles/SB10001424052702304610404579405021384734070.

[2] European Commission, last update 12 March 2014. *Reducing CO2 emissions from passenger cars*, viewed 8 March 2014, http://ec.europa.eu/clima/policies/transport/vehicles/-cars/index_en.htm.

[3] International Council On Clean Transportation. European CO2 Emission Performance Standards for Passenger Cars and light Commercial Vehicles. *Policy Update*, p. 5, 2012.

[4] Volkswagen 2014. 'The new Volkswagen XL1 Super Efficient Vehicle (SEV)', viewed 10 March 2014, http://www.volkswagen.co.uk/about-us/futures/xl1.

[5] M. Hou and K. Friedrich. 3-D Stamp Forming of Thermoplastic Matrix Composites, *Applied Composite Materials*, 1:135-153, 1994.

[6] T. C. Lim, S. Ramakrishna, H. M. Shang. Axisymmetric sheet forming of knitted fabric composite by combined stretch forming and deep drawing, *Composites Part B: Engineering*, 30:495–502, 1999.

[7] S. Davey, R. Das, W.J. Cantwell, S. Kalyanasundaram. Forming studies of carbon fibre composite sheets in dome forming processes, *Composite Structures*, 97: 310–316, 2013.

[8] W. Wang, A. Lowe, S. Kalyanasundaram. A study on continuous flax fibre reinforced polypropylene composite in stamp forming process. *Advanced Composites Letters*, 22:86-89, 2013.

[9] N.O. Cabrera, C.T. Reynolds, B. Alcock, T. Peijs. Non-isothermal stamp forming of continuous tape reinforced all-polypropylene composite sheet, *Composites: Part A*, 39:1455–1466, 2008.

[10] L. Mosse, P. Compston, W. J. Cantwell, M. Cardew-Hall, S. Kalyanasundaram. Stamp forming of polypropylene based fibre–metal laminates: The effect of process variables on formability, *Journal of Materials Processing Technology*, 172:163-168, 2006.

[11] L. Mosse, P. Compston, W. J. Cantwell, M. Cardew-Hall, S. Kalyanasundaram. The effect of process temperature on the formability of polypropylene based fibre–metal laminates, *Composites: Part A*, 36:1158–1166, 2005.

[12] L. Mosse, P. Compston, W. J. Cantwell, M. Cardew-Hall, S. Kalyanasundaram. The development of a finite element model for simulating the stamp forming of fibre–metal, laminates, *Composite Structures*, 75:298-304, 2006.

[13] J. Gresham, W. Cantwell, M.J. Cardew-Hall, P. Compston, S. Kalyanasundaram. Drawing behaviour of metal–composite sandwich structures, *Composite Structures*, 75:305–312, 2006.

[14] P. Compston, W. J. Cantwell, M.J. Cardew-Hall, S. Kalyanasundaram, L. Mosse. Comparison of surface strain for stamp formed aluminum and an aluminum-polypropylene laminate, *Journal of Materials Science*, 39:6087-6088, 2004.

[15] A. Sexton, W. Cantwell, S. Kalyanasundaram. Stretch forming studies on a fibre metal laminate based on a self-reinforcing polypropylene composite, *Composite Structures*, 94:431-437, 2012.

[16] S. Kalyanasundaram, S. DharMalingam, S. Venkatesan, A. Sexton. Effect of process parameters during forming of self reinforced – PP based Fiber Metal Laminate, *Composite Structures*, 97:332-337, 2013.